A Flexible One-node CMFD Algorithm for Multi-group Diffusion and SP_3 Equations in Hexagonal Geometry

Seongdong Jang, Woong Heo, and Yonghee Kim*
Korea Advanced Institute of Science and Technology (KAIST)
291 Daehak-ro, Yuseong-gu, Daejeon, 34141, Republic of Korea
**Corresponding author: yongheekim@kaist.ac.kr*

1. Introduction

In general, the Boltzmann neutron transport equation is approximated as a diffusion and SP_3 theory due to the limitations of the computational efficiency. In terms of computational acceleration, Coarse-Mesh Finite Difference (CMFD) algorithm is very popular for the diffusion and SP_3 theory [1-2]. One of the efficient acceleration method is the one-node CMFD [3-4].

The efficiency of the one-node CMFD algorithm is coming from the parallel calculation. In the hexagonal geometry, the hexagonal coarse mesh Finite Difference Method (FDM) is calculated by updated correction factors, which can be obtained from the triangular fine mesh FDM as a high fidelity solution. To improve computational efficiency, the triangular fine mesh FDM can be solved separately.

In this paper, the flexible one-node CMFD algorithm is introduced for the multi-group diffusion and SP_3 equations in hexagonal geometry. The key idea of the flexible one-node CMFD is that the computational efficiency can be maximized if the different number of the triangular fine meshes are introduced, depending on the characteristic of the reactor core.

2. Methodology

As shown in Fig. 1, there are three steps for the flexible one-node CMFD algorithm for the diffusion and SP_3 analysis which are the global hexagonal CMFD calculation, the local triangular fine mesh FDM calculation, and the correction factor calculation.

In the first step, the eigenvalue problem is solved for the hexagonal CMFD with the updated correction factors, calculated from the previous iteration. The modulated partial currents and modulated node average flux, or moments, can be obtained by combining inaccurate solutions from the global calculation step with the shape functions from the local calculation step.

In the local calculation step, the balance equations are defined as a fixed source problem with the incoming partial current boundary conditions. The fixed source is coming from the modulated node average flux, or moments, and the multiplication factor. The boundary condition are obtained using the modulated incoming partial currents. For the high fidelity solution, the hexagonal node is divided into identical triangular fine meshes.

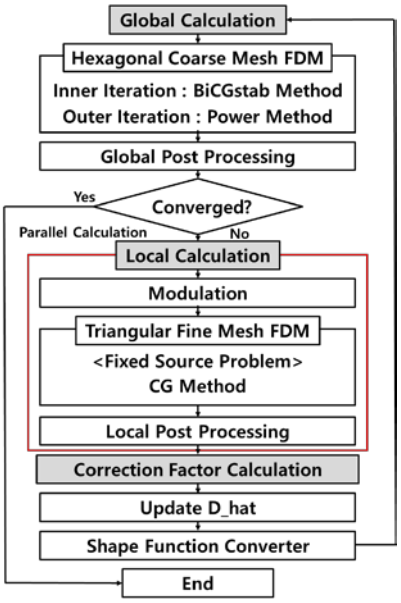

Fig. 1. Algorithm scheme of the flexible one-node CMFD

Using the high fidelity solution, the correction factor can be updated. The only difference between one-node CMFD and flexible one-node CMFD algorithm schemes is that the shape function converter step, which is conducted after the correction factor update step. In this step, the shape function of the outgoing partial current is converted to that of the adjacent hexagonal node, which has the different number of triangular meshes.

Especially, in the case of SP_3 one-node CMFD, numerical instability is occurred due to the second order moments, therefore the Flux-level-fixup CMFD (FF-CMFD) method is applied.

2.1. Global Calculation

There are two correction factors at the surface of the global hexagonal nodes for diffusion analysis as shown in Fig. 2. On the other hand, the four correction factors are needed for SP_3 analysis.

Due to the correction factors, the system matrix of the global hexagonal CMFD is asymmetric. For solving the diffusion and SP_3 eigenvalue equations, the Bi-conjugate Gradient Stabilized (BiCGstab) method is used for inner-iteration and the power method is used for the outer-iteration.

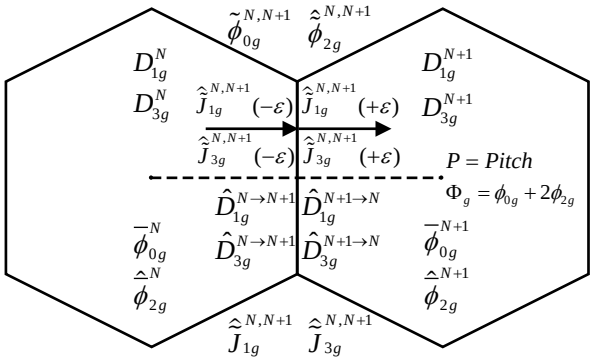

Fig. 2. Hexagonal geometry for global calculation

In case of SP_3 analysis, the net currents can be defined with the biased second order moments as below:

$$\tilde{J}_{1g}^{N,N+1}(-\varepsilon) = -D_{1g}^{N}\frac{\tilde{\Phi}_g^{N,N+1} - \bar{\Phi}_g^{N}}{p/2} - \hat{D}_{1g}^{N\to N+1}\frac{\tilde{\Phi}_g^{N,N+1} + \bar{\Phi}_g^{N}}{p/2} \quad (1)$$

$$\tilde{J}_{1g}^{N,N+1}(+\varepsilon) = -D_{1g}^{N+1}\frac{\bar{\Phi}_g^{N+1} - \tilde{\Phi}_g^{N,N+1}}{p/2} + \hat{D}_{1g}^{N+1\to N}\frac{\tilde{\Phi}_g^{N,N+1} + \bar{\Phi}_g^{N+1}}{p/2} \quad (2)$$

$$\tilde{J}_{3g}^{N,N+1}(-\varepsilon) = -D_{3g}^{N}\frac{\tilde{\phi}_{2g}^{N,N+1} - \bar{\phi}_{2g}^{N}}{p/2} - \hat{D}_{3g}^{N\to N+1}\frac{\tilde{\phi}_{2g}^{N,N+1} + \bar{\phi}_{2g}^{N}}{p/2} \quad (3)$$

$$\tilde{J}_{3g}^{N,N+1}(+\varepsilon) = -D_{3g}^{N+1}\frac{\bar{\phi}_{2g}^{N+1} - \tilde{\phi}_{2g}^{N,N+1}}{p/2} + \hat{D}_{3g}^{N+1\to N}\frac{\tilde{\phi}_{2g}^{N,N+1} + \bar{\phi}_{2g}^{N+1}}{p/2} \quad (4)$$

By continuity condition, the net currents can be rewritten as below:

$$\begin{aligned}\hat{\tilde{J}}_{1g}^{N,N+1} = &-\frac{2}{p}\frac{(D_{1g}^{N} + \hat{D}_{1g}^{N\to N+1})(D_{1g}^{N+1} - \hat{D}_{1g}^{N+1\to N})}{D_{1g}^{N} + D_{1g}^{N+1} + \hat{D}_{1g}^{N\to N+1} + \hat{D}_{1g}^{N+1\to N}}\hat{\bar{\Phi}}_g^{N+1} \\ &+\frac{2}{p}\frac{(D_{1g}^{N} - \hat{D}_{1g}^{N\to N+1})(D_{1g}^{N+1} + \hat{D}_{1g}^{N+1\to N})}{D_{1g}^{N} + D_{1g}^{N+1} + \hat{D}_{1g}^{N\to N+1} + \hat{D}_{1g}^{N+1\to N}}\hat{\bar{\Phi}}_g^{N}\end{aligned} \quad (5)$$

$$\begin{aligned}\hat{\tilde{J}}_{3g}^{N,N+1} = &-\frac{2}{p}\frac{(D_{3g}^{N} + \hat{D}_{3g}^{N\to N+1})(D_{3g}^{N+1} - \hat{D}_{3g}^{N+1\to N})}{D_{3g}^{N} + D_{3g}^{N+1} + \hat{D}_{3g}^{N\to N+1} + \hat{D}_{3g}^{N+1\to N}}\hat{\bar{\phi}}_{2g}^{N+1} \\ &+\frac{2}{p}\frac{(D_{3g}^{N} - \hat{D}_{3g}^{N\to N+1})(D_{3g}^{N+1} + \hat{D}_{3g}^{N+1\to N})}{D_{3g}^{N} + D_{3g}^{N+1} + \hat{D}_{3g}^{N\to N+1} + \hat{D}_{3g}^{N+1\to N}}\hat{\bar{\phi}}_{2g}^{N}\end{aligned} \quad (6)$$

For the boundary conditions, the albedo boundary condition is applied, to consider the vacuum and reflective boundary condition.

2.2. Local Calculation

The modulated partial currents and the modulated node average flux, or moments, are calculated by the magnitude and the shape functions. The magnitude can be obtained from the global calculation step and the shape functions can be calculated from the previous local calculation step.

Using the modulated incoming partial current boundary condition, the fixed source diffusion and SP_3 equations can be solved by Conjugate Gradient (CG) method. The fixed source can be determined by modulated node average flux or moments, and multiplication factor.

2.3. Correction factor update

The correction factors can be calculated from the high fidelity solutions, reference net current and reference surface flux as below:

$$\hat{D}_{1g}^{N\to N+1} = \left(-\frac{p}{2}\hat{\tilde{J}}_{1g}^{N,N+1}(-\varepsilon) - D_{1g}^{N}(\hat{\tilde{\Phi}}_g^{N,N+1} - \hat{\bar{\Phi}}_g^{N})\right) / \left(\hat{\tilde{\Phi}}_g^{N,N+1} + \hat{\bar{\Phi}}_g^{N}\right) \quad (7)$$

$$\hat{D}_{1g}^{N+1\to N} = \left(\frac{p}{2}\hat{\tilde{J}}_{1g}^{N,N+1}(+\varepsilon) + D_{1g}^{N+1}(\hat{\bar{\Phi}}_g^{N+1} - \hat{\tilde{\Phi}}_g^{N,N+1})\right) / \left(\hat{\tilde{\Phi}}_g^{N,N+1} + \hat{\bar{\Phi}}_g^{N+1}\right) \quad (8)$$

$$\hat{D}_{3g}^{N\to N+1} = \left(-\frac{p}{2}\hat{\tilde{J}}_{3g}^{N,N+1}(-\varepsilon) - D_{3g}^{N}(\hat{\tilde{\phi}}_{2g}^{N,N+1} - \hat{\bar{\phi}}_{2g}^{N})\right) / \left(\hat{\tilde{\phi}}_{2g}^{N,N+1} + \hat{\bar{\phi}}_{2g}^{N}\right) \quad (9)$$

$$\hat{D}_{3g}^{N+1\to N} = \left(\frac{p}{2}\hat{\tilde{J}}_{3g}^{N,N+1}(+\varepsilon) + D_{3g}^{N+1}(\hat{\bar{\phi}}_{2g}^{N+1} - \hat{\tilde{\phi}}_{2g}^{N,N+1})\right) / \left(\hat{\tilde{\phi}}_{2g}^{N,N+1} + \hat{\bar{\phi}}_{2g}^{N+1}\right) \quad (10)$$

2.4. Shape function converter

To explain the converted shape function, the side Division Mode (DM) is defined as a number of triangular meshes at the side of the hexagonal node. For instance, the DM of LHS hexagonal node is 4 and that of RHS is 3 as shown in Fig. 3. The key idea of the shape function converting procedure is that the fictitious cells are introduced, which are generated by the number of cells created as common multiple, between the DM from each hexagonal node.

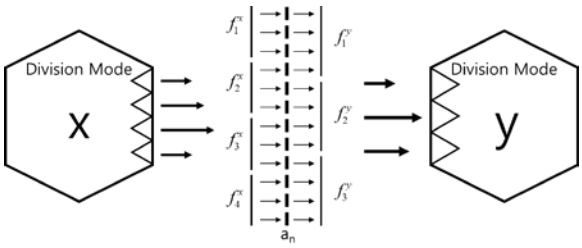

Fig. 3. Outgoing partial current shape function converter

Using the fictitious cell, the converted shape functions can be generated as weighted average shape functions, as below:

$$f_i^{y} = \frac{1}{x}\sum_{j=1}^{y} a_{j+(i-1)y} \quad (11)$$

Although a higher order fitting method is needed when the converted shape function is generated from the lower to higher DM, the linear fitting is considered in this paper.

3. Numerical Results

To analyze the flexible one-node CMFD algorithm for multi-group diffusion and SP_3 equations, a 2-D prototype Gen-IV (PGSFR) was considered as shown in Fig. 4. The 9G and 24G homogenized cross section were used to consider the multi-group calculation. In this study, the primary control assemblies were inserted in the active core region and the homogeneous mixture of sodium and duct was filled in the secondary control assembly region.

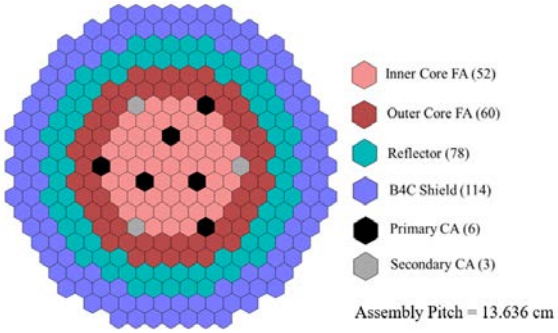

Fig. 4. PGSFR core configuration

The reference multiplication factors were calculated with 1E-8 for eigenvalue tolerance and 1E-7 for fission source tolerance using the highest DM as shown in Table I.

Table I: Reference Multiplication Factors

	9G		24G	
	A* (50)	B** (50)	A* (30)	B** (30)
k_{eff}	1.154962	1.159502	1.151893	1.156485

** Diffusion Analysis (DM), **SP_3 Analysis (DM)*

For the flexible one-node CMFD, the different DMs were defined as shown in Fig. 5. The strategy of defining different DMs was that the maximum DM was designated at the boundary and primary control rod assembly node, and it was decreased continuously to the adjacent hexagonal nodes.

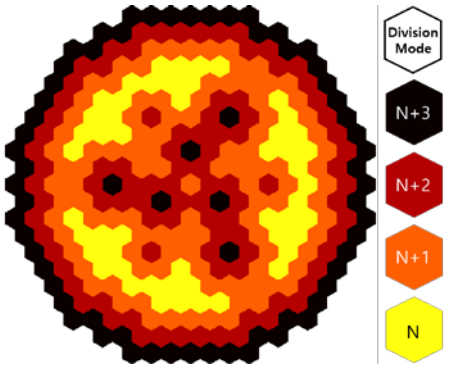

Fig. 5. Strategy of defining different DM

To compare the performance of one-node CMFD and flexible one-node CMFD, every calculating condition was fixed, except for the number of triangular mesh per hexagon in terms of the DM. Every calculation were conducted with OpenMP parallel calculation using 40 cores of the Intel® Xeon® Gold 6148 CPU @ 2.40GHz. The convergence tolerances were same with the reference calculation. To enhance the convergence behavior, the number of local calculations, which are called sweeping, were fixed, 2 for diffusion analysis and 3 for SP_3 analysis.

As increasing the DM, the multiplication factors were converged to the reference solution. The absolute error was plotted depending on the DM and computing time. The case of the 9G analysis is shown in Fig. 6.

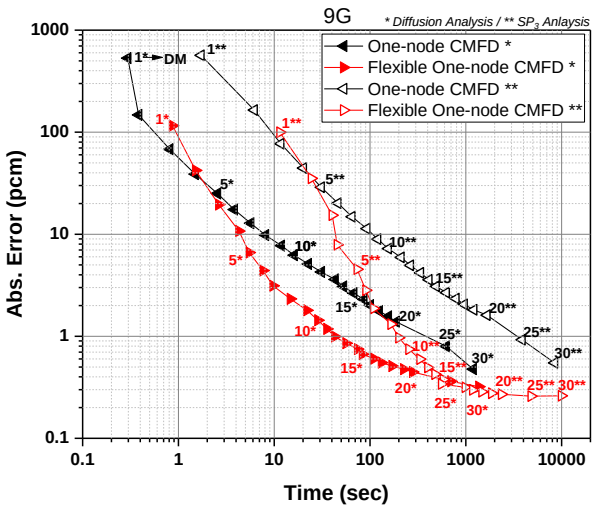

Fig. 6. Absolute error depending on computing time

To compare the efficiency, the computing times are tabulated, where absolute errors are 10, 5 and 1 pcm as shown in Table II. These computing times were calculated by interpolation. For instance, the actual computing times and absolute error, (187.20 sec, 1.39 pcm) and (625.67 sec, 0.80 pcm), were used to expect the virtual computing time 475.28 sec when the absolute error is 1 pcm in case of 9G one-node CMFD diffusion analysis.

Table II: Computing Time

		Diffusion Analysis		SP_3 Analysis	
Abs. Err. Accuracy (pcm)		A* (sec)	B** (sec)	A* (sec)	B** (sec)
9G	10	7.95	4.50	108.10	44.07
	5	23.77	7.07	261.11	69.54
	1	475.28	42.64	3622.46	196.68
24G	10	21.55	8.19	291.88	107.27
	5	64.03	13.17	577.27	133.18
	1	2272.06	45.54	10528.32	256.59

** One-node CMFD, ** Flexible One-node CMFD*

The results show that the convergence behavior of the flexible one-node CMFD has tremendous efficiency compared with those of one-node CMFD. Even though those results of one-node CMFD are coming from the parallel calculation with high efficiency, it is totally inefficient when it is compared with the efficiency of the results from the flexible one-node CMFD.

The normalized power distributions were calculated where absolute error of their multiplication factors were ~ 1 pcm, as shown in Fig. 7~10.

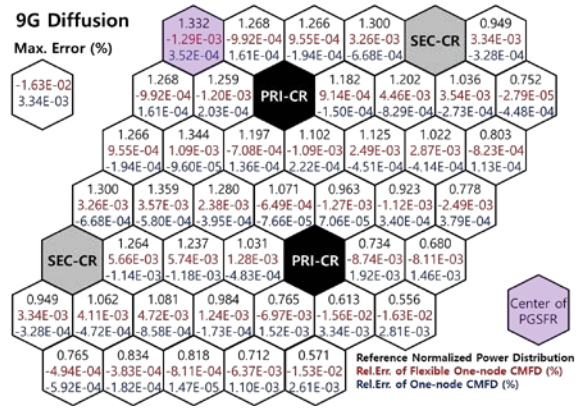

Fig. 7. Normalized power distribution of 9G diffusion analysis

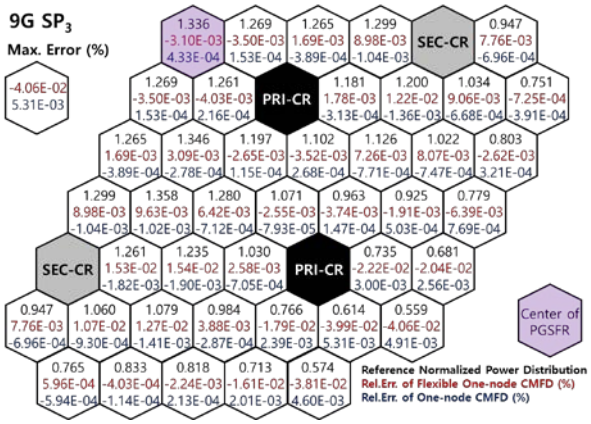

Fig. 8. Normalized power distribution of 9G SP_3 analysis

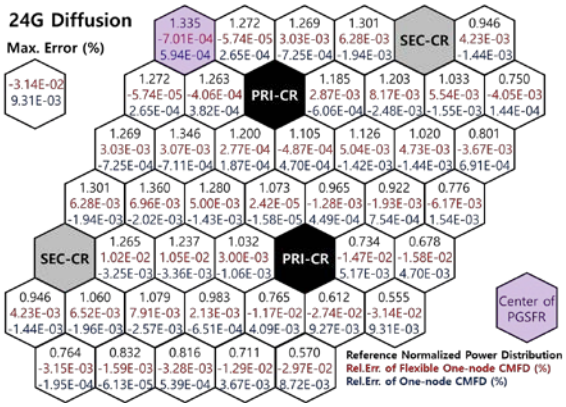

Fig. 9. Normalized power distribution of 24G diffusion analysis

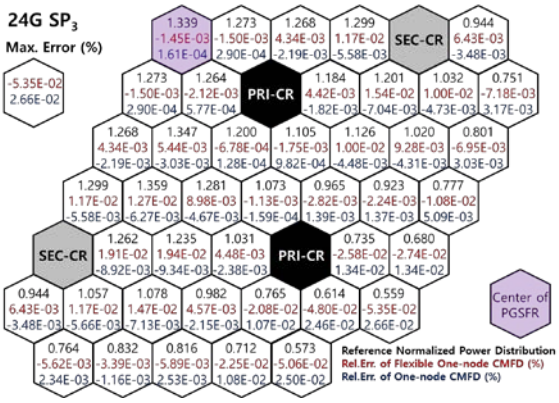

Fig. 10. Normalized power distribution of 24G SP_3 analysis

The results show that the normalized power error of the flexible one-node CMFD is acceptable, although lower DM, which means relative coarse mesh, is used. Due to the converted shape function as a linear fitting, its effectiveness had been doubtful when it is converted from the lower order to the higher order DM. However, the results show that it is very effective if continuous DMs are used at the interface.

4. Conclusion

The flexible one-node CMFD algorithm is successfully applied to the multi-group diffusion and SP_3 equations for the hexagonal geometry. It is concluded that the efficiency of the flexible one-node CMFD is much higher than that of one-node CMFD. Although the lower division mode (DM) and linear fitting for converted shape function are used, it is demonstrated that the accuracy of the normalized power distribution of flexible one-node CMFD is guaranteed.

ACKNOWLEDGMENTS

This work was supported by the National Research Foundation of Korea (NRF) Grant funded by the Korean Government (MSIP) (NRF-2016R1A5A1013919).

REFERENCES

[1] K. S. Smith, “Nodal Method Storage Reduction by Non-linear Iteration,” Trans. Am. Nucl. Soc., 44, pp. 265 (1983).
[2] A. Yamamoto, T. Sakamoto and T. Endo, “A CMFD Acceleration Method for SP_3 Advanced Nodal Method,” Nucl. Sci. Eng. 184(2), pp. 167-173 (2016)
[3] H. C. Shin, Y. H. Kim, Y. B. Kim and S. M. Bae, “A Nonlinear Combination of CMFD (Coarse-Mesh finite Difference) and FMFD (Fine-Mesh Finite Difference) Methods,” Proceedings of the Korean Nuclear Society Spring Meeting, Pohang, South Korea, May, 1999 (1999)
[4] S. D. Jang and Y. H. Kim. “One-node CMFD formulations for multi-group SP_3 equations in hexagonal geometry,” proceeding of the PHYSOR 2018, Cancun, Mexico, April, 2018 (2018)